

# Stabilizing the surface morphology of $\text{Si}_{1-x-y}\text{Ge}_x\text{C}_y/\text{Si}$ heterostructures grown by molecular beam epitaxy through the use of a silicon-carbide source

E. T. Croke,<sup>a)</sup> J. J. Vajo, and A. T. Hunter  
*HRL Laboratories, LLC, 3011 Malibu Canyon Road, RL63, Malibu, California 90265*

C. C. Ahn  
*California Institute of Technology, Pasadena, California 91125*

D. Chandrasekhar, T. Laursen, David J. Smith, and J. W. Mayer  
*Center for Solid State Science, Arizona State University, Tempe, Arizona 85287-1704*

(Received 9 September 1997; accepted 18 May 1998)

$\text{Si}_{1-x-y}\text{Ge}_x\text{C}_y/\text{Si}$  superlattices were grown by solid-source molecular beam epitaxy using silicon carbide as a source of C. Samples consisting of alternating layers of nominally 25 nm  $\text{Si}_{1-x-y}\text{Ge}_x\text{C}_y$  and 35 nm Si for 10 periods were characterized by high-resolution x-ray diffraction, transmission electron microscopy (TEM), and Rutherford backscattering spectrometry to determine strain, thickness, and composition. C resonance backscattering and secondary ion mass spectrometries were used to measure the total C concentration in the  $\text{Si}_{1-x-y}\text{Ge}_x\text{C}_y$  layers, allowing for an accurate determination of the substitutional C fraction to be made as a function of growth rate for fixed Ge and substitutional C compositions. For C concentrations close to 1%, high-quality layers were obtained without the use of Sb-surfactant mediation. These samples were found to be structurally perfect to a level consistent with cross-sectional TEM ( $<10^7$  defects/cm<sup>2</sup>) and showed considerably improved homogeneity as compared with similar structures grown using graphite as the source for C. For higher Ge and C concentrations, Sb-surfactant mediation was found to be required to stabilize the surface morphology. The maximum value of substitutional C concentration, above which excessive generation of stacking fault defects caused polycrystalline and/or amorphous growth, was found to be approximately 2.4% in samples containing between 25 and 30% Ge. The fraction of substitutional C was found to decrease from roughly 60% by a factor of 0.86 as the  $\text{Si}_{1-x-y}\text{Ge}_x\text{C}_y$  growth rate increased from 0.1 to 1.0 nm/s. © 1998 American Vacuum Society. [S0734-211X(98)06804-8]

## I. INTRODUCTION

We report developments in the growth of  $\text{Si}_{1-x-y}\text{Ge}_x\text{C}_y/\text{Si}$  heterostructures that are now making high-quality material available for device fabrication. A promising picture is beginning to emerge that includes the possibility of achieving large band-gap differences between Si and  $\text{Si}_{1-x-y}\text{Ge}_x\text{C}_y$  lattice matched to a Si substrate.<sup>1-3</sup> These developments, if realized, would allow for further advancements in heterojunction bipolar transistor (HBT) technologies<sup>4,5</sup> based on Group IV elements, since reliability issues relating to the increased strain in high-Ge content, SiGe HBTs can, in principle, be minimized or eliminated using  $\text{Si}_{1-x-y}\text{Ge}_x\text{C}_y$ .<sup>6,7</sup> Furthermore, the picture also includes the possibility of achieving significant conduction band offsets for  $\text{Si}_{1-x-y}\text{Ge}_x\text{C}_y$  coherently strained or lattice matched to a Si substrate.<sup>3</sup> Together with  $\text{Si}_{1-x}\text{Ge}_x$  or compressively strained  $\text{Si}_{1-x-y}\text{Ge}_x\text{C}_y$ , complementary metal-oxide-semiconductor (MOS) devices consisting of high-mobility field effect transistors involving both *n*- and *p*-type two-dimensional carrier gas (2DCG) structures are envisioned.<sup>8,9</sup> A  $\text{Si}_{1-x-y}\text{Ge}_x\text{C}_y$ -based approach might, there-

fore, allow for implementation of next-generation, high-speed CMOS at integration levels consistent with state-of-the-art Si device processing capabilities.

Fundamentally, we are interested in understanding the maximum amount of Ge and C that can be substitutionally incorporated into  $\text{Si}_{1-x-y}\text{Ge}_x\text{C}_y$  in a manner consistent with the growth of device-quality material. We have shown that the use of an e-beam-sublimated graphite source in the molecular beam epitaxy (MBE) of  $\text{Si}_{1-x-y}\text{Ge}_x\text{C}_y$  leads to a rough surface morphology and inhomogeneous incorporation for Ge and C concentrations as low as 9% and 1%, respectively.<sup>10</sup> This surface instability was observed to worsen for thicker films, depending on the Ge and C fractions, limiting either the concentrations or the thickness to very low (impractical) levels. Believing that the limitations were due to the presence of immobile molecules of C<sub>2</sub> and C<sub>3</sub> on the surface, we began experimenting with the use of Sb as a surfactant.<sup>11</sup> We discovered that much higher concentrations of both Ge and C (23% and 1.8%, respectively) could be reached in arbitrarily thick layers of defect-free material.<sup>12</sup>

In this article, we present new results which we have obtained through the use of an e-beam-sublimated silicon-carbide (SiC) source for C. The C source substantially

<sup>a)</sup>Electronic mail: croke@hrl.com

TABLE I.  $\text{Si}_{1-x-y}\text{Ge}_x\text{C}_y/\text{Si}$  superlattice sample set (10 periods each).

Sample <sup>a</sup>	Sb Coverage	$r_{\text{SiGeC}}$ (nm/s)	HRXRD/RBS/CRBS					SIMS		$C_s/C_t^d$ (%)
			$T_{\text{Si}}$ (nm)	$T_{\text{SiGeC}}$ (nm)	%Ge	%C <sub>s</sub>	%C <sub>t</sub>	%Ge	%C <sub>t</sub>	
HA96.017	0 ML	0.23	33.0	24.0	10.8	0.9	N/D	N/D	N/D	N/D
HA97.020	0 ML	0.24	35.0	25.0	9.6	1.3	1.9	N/D	1.3 <sup>b</sup>	66 ± 42
HA97.055	0.5 ML	0.16	38.5	27.5	23.4	2.2	3.6	N/D	N/D	61 ± 21
HA97.106	0.5 ML	0.09	33.0	22.0	30.6	2.2	3.5	31 <sup>c</sup>	3.4 <sup>c</sup>	62 ± 22
HA97.111	0.5 ML	0.48	35.0	23.5	29.3	2.4	4.2	28 <sup>c</sup>	4.3 <sup>c</sup>	56 ± 17
HA97.115	0.5 ML	1.02	33.5	25.0	25.6	2.2	4.4	24 <sup>c</sup>	4.1 <sup>c</sup>	51 ± 14

<sup>a</sup>Samples HA96.017 and HA97.020 were each grown at 450 °C. Samples HA97.055, .106, .111, and .115 were grown at 500 °C.

<sup>b</sup>SIMS calibration of %C<sub>t</sub> in sample HA97.020 was determined using sensitivity factors derived from a comparison of HRXRD/RBS/CRBS and SIMS data taken from samples HA97.020 and HA97.055, adjusting for changes in matrix due to the different Ge concentrations.

<sup>c</sup>SIMS calibration of samples HA97.106, .111, and .115 was based on HRXRD/RBS/CRBS analysis of HA97.055.

<sup>d</sup>The ratio C<sub>s</sub>/C<sub>t</sub> was calculated from the values obtained from the HRXRD/RBS/CRBS analysis.

changes the nature of the molecular species reaching the growing  $\text{Si}_{1-x-y}\text{Ge}_x\text{C}_y$  layers. We will show that for 9.6% Ge and 1.3% C, use of the SiC source results in homogeneous incorporation of Ge and C, a significant improvement over the results obtained previously with our graphite source. We will also present results from characterizations of  $\text{Si}_{1-x-y}\text{Ge}_x\text{C}_y/\text{Si}$  superlattices of varying Ge and C concentrations in excess of 10% and 1%, respectively, grown using our SiC source. We have used high-resolution x-ray diffraction (HRXRD) to measure the period and the average strain of the superlattices, Rutherford backscattering (RBS), C resonance backscattering (CRBS), and secondary ion mass spectrometries (SIMS) to measure the Ge and C concentrations, and transmission electron microscopy (TEM) to study the microstructural detail. We also present data showing the maximum amounts of Ge and C that can be grown defect-free using this source, including the results of experiments involving Sb-surfactant mediation, and compare these results with those previously obtained using the graphite source. Finally, we describe an analysis of HRXRD, RBS, and CRBS data that, taken together, provide an estimate of the fraction of substitutional C present in the samples as a function of  $\text{Si}_{1-x-y}\text{Ge}_x\text{C}_y$  growth rate.

## II. EXPERIMENT

Several  $\text{Si}_{1-x-y}\text{Ge}_x\text{C}_y/\text{Si}$  superlattices were grown for this study in a Perkin-Elmer (Model 430S) Si MBE system (base pressure  $< 1 \times 10^{-10}$  Torr) designed for solid-source deposition onto heated, 5 in. Si substrates. Source materials consisting of a shaped Si charge, Ge chunks, and a 0.25-in.-thick SiC wafer (obtained from CREE Research, Inc.) were loaded into each of three Temescal electron-beam evaporators. In the case of Ge, a graphite crucible liner was used to provide enhanced stability and more uniform heating than would otherwise be possible if the Ge were placed directly into the copper hearth. For the SiC, a special graphite holder was designed to minimize thermal contact with the hearth

and provide a method for containing the pieces of SiC that would inevitably break off from the original wafer during use.

### A. $\text{Si}_{1-x-y}\text{Ge}_x\text{C}_y/\text{Si}$ sample set

(100) Si substrates were prepared *ex situ* by spinning them to 4000 rpm in a Laurell Technologies polypropylene spinner (Model WS-200-4NPP/RV) and pouring 5% HF [1:10 dilution in de-ionized (DI) water] over the polished surface until they became hydrophobic. After a short rinse (5 s in DI water), the wafers were loaded into a buffer chamber and then into the growth chamber. Prior to deposition, the substrates were heated to 850 °C and exposed to a 0.01 nm/s Si flux,<sup>13</sup> in order to remove any oxide contamination remaining from the HF etching process. Wafers prepared in this manner exhibited a clean (2×1)-reconstructed surface, as observed with reflection high-energy electron diffraction (RHEED). Following oxide desorption, the substrate temperatures were reduced to either 450 or 500 °C and a Si buffer layer was grown, typically to a thickness on the order of 50–100 nm. After growth of the buffer layer and prior to deposition of the superlattices, some samples received 1/2 monolayer (ML) predeposit of Sb, to reduce surface diffusion rates, allowing for more uniform incorporation and the preservation of an atomically smooth growth front. Finally, 10-period superlattices, consisting of nominally 25 nm  $\text{Si}_{1-x-y}\text{Ge}_x\text{C}_y/35$  nm Si in each bilayer, were grown under various conditions in order to study crystalline quality and substitutional C fraction as a function of composition and growth rate. Growth parameters (temperature and Sb coverage prior to the start of superlattice growth) and results from HRXRD/RBS/CRBS and SIMS characterizations are shown in Table I.

### B. SiC vs graphite sources for C deposition

SiC was chosen as a source for C due to the expectation that the nature of the depositing species would change considerably, as compared with use of a graphite source.<sup>14</sup> In a

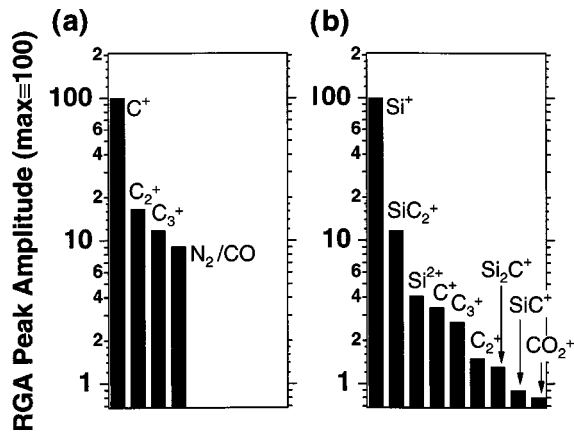


FIG. 1. Relative RGA peak amplitudes for (a) graphite vs (b) silicon-carbide sources. RGA peak amplitude for various constituents generated through e-beam sublimation of graphite and silicon carbide are presented. The data are shown relative the major component (set equal to 100) in each source.

previous paper,<sup>12</sup> we showed that high-quality, homogeneous,  $\text{Si}_{1-x-y}\text{Ge}_x\text{C}_y$  layers could be grown using a graphite source for substitutional C concentrations approaching 2%, provided that the growth was Sb mediated. Without Sb mediation, even for layers in which the Ge and C concentrations were only 10% and 1%, respectively, we observed roughening of the  $\text{Si}_{1-x-y}\text{Ge}_x\text{C}_y$  surface and evidence of inhomogeneous lateral incorporation. Through the use of the SiC source, we expected to deposit molecular species that contained both Si and C,<sup>14</sup> rather than just C, and hence improve the homogeneity and perhaps, stabilize the surface morphology in the process.

While the SiC source was hot, we scanned, using a residual gas analyzer (RGA), over masses ranging from amu 2 ( $\text{H}_2$ ) to amu 75, in order to characterize the species that sublimated from the source under typical operating conditions. These scans were compared with scans obtained under base vacuum conditions (i.e., sources cold,  $\text{LN}_2$  shrouds cold, and cryopump on and pumping) and with those obtained previously using a graphite source. The results are shown in Fig. 1. The data were normalized so that the amplitude of the RGA signal for the major constituent in each source was set equal to 100. For the graphite source, monomeric C (amu 12) appears as the peak with the largest signal amplitude but contributions from  $\text{C}_2$  (amu 24) and  $\text{C}_3$  (amu 36) were also significant. In comparison, the major constituent sublimating from the SiC source, was found to be Si, although we also observed  $\text{SiC}_2$  and, to a lesser extent, C,  $\text{C}_2$ , and  $\text{C}_3$ . Closed-loop control of the SiC source (and approximately, the amount of C contained in the flux) was achieved by tuning the RGA to amu 52 ( $\text{SiC}_2$ ) and automatically adjusting the power to the electron gun with a computer to maintain a predetermined setpoint value.

### C. Method for computing sample composition from HRXRD, RBS, and TEM

Superlattice composition and layer thicknesses were calculated from data obtained from a combination of measure-

ments involving HRXRD, RBS, CRBS, and TEM. Four pieces of information were required, in addition to the shutter opening and closing times, to uniquely determine the structure. We used HRXRD to provide the average strain and superlattice period, RBS to measure the average Ge concentration, and TEM lattice imaging to obtain the Si layer thickness. From these data, the four relevant fluxes, identified as (1) Si from the primary Si source, (2) Si from the SiC source, (3) Ge, and (4) C, were calculated assuming unity sticking coefficient for the various constituents in a manner consistent with Vegard's Law and the lattice constants for Si, Ge, and  $\beta$ -SiC. Finally, from the fluxes and the shutter opening and closing times, we calculated the layer thickness and composition of the  $\text{Si}_{1-x-y}\text{Ge}_x\text{C}_y$  layers. CRBS was used to determine the total C concentration ( $\%C_t$  in Table I), since only the substitutional C concentration,  $y$  ( $\%C_s$  in Table I), could be accessed by the above method. The ratio,  $\%C_s/\%C_t$ , also shown in Table I, therefore represents the percentage of incorporated C contributing to the strain.

(004) HRXRD spectra were obtained by collimating Cu  $K\alpha$  radiation, selected through the aid of a four-crystal Ge monochromator, onto each sample in a  $\theta$ - $2\theta$  geometry. The spectra generally consisted of a Si substrate peak at  $34.5644^\circ$  and a series of superlattice peaks. Analysis of superlattice period and average strain followed the method of Speriosu and Vreeland.<sup>15</sup> Standard 2 MeV  $\text{He}^{2+}$  backscattering was used for probing Si and Ge, whereas 4.3 MeV  $\text{He}^{2+}$  C-resonance backscattering probed the C component. These ion backscattering techniques were used to measure the average Ge and C concentrations, since individual layers could not be resolved. The estimated uncertainties associated with the RBS and CRBS measurements were  $\pm 0.5$  at. % for both the average Ge and average C concentrations.

SIMS characterization was performed immediately after each growth to provide a convenient method for verifying sample composition from run to run. The analysis system consisted of a Perkin-Elmer (Model 595) Auger Microprobe equipped with a 3500 SIMS II attachment. A 2 keV  $\text{O}_2^+$  primary beam was sufficient to resolve each individual  $\text{Si}_{1-x-y}\text{Ge}_x\text{C}_y$  layer. The sample HA97.055 was used as a calibration standard as it had been previously characterized by HRXRD/RBS/CRBS.

## III. RESULTS AND DISCUSSION

### A. TEM micrographs compare growth using graphite vs SiC sources

In Fig. 2, we compare cross-sectional TEM micrographs obtained from two  $\text{Si}_{0.90}\text{Ge}_{0.10}\text{C}_{0.01}/\text{Si}$  superlattice samples grown without the benefit of Sb mediation. The images were taken on a Philips EM430 operated at 200 keV using a (400) two-beam condition near a  $[011]$  zone axis. The sample on the left side of the figure (HA96.017) was grown using a graphite source, while the sample on the right (HA97.020) was grown using the SiC source. The micrograph of HA96.017 shows contrast *within* the  $\text{Si}_{1-x-y}\text{Ge}_x\text{C}_y$  layers, suggesting that incorporation was laterally inhomogeneous. HA97.020 shows no such contrast and reveals the layers to

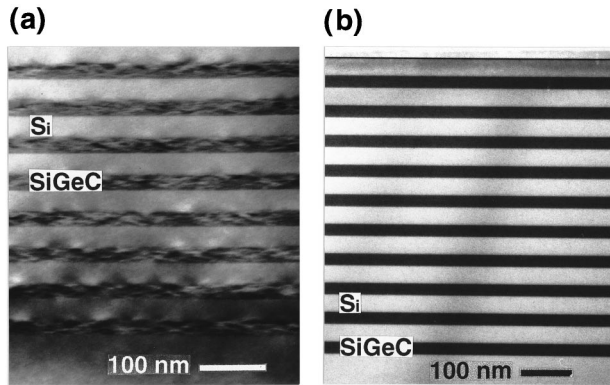


FIG. 2. Cross-sectional TEM micrographs compare a superlattice grown using the graphite source vs a superlattice grown using the silicon-carbide source. (a) Graphite source: HA96.017 240 Å  $\text{Si}_{0.883}\text{Ge}_{0.108}\text{C}_{0.009}/330$  Å Si (no Sb-mediation); (b) silicon-carbide source: HA97.020 250 Å  $\text{Si}_{0.891}\text{Ge}_{0.096}\text{C}_{0.013}/350$  Å Si (no Sb-mediation). Significant improvement of homogeneity and interface abruptness due to the use of a silicon-carbide source are demonstrated for two  $\text{Si}_{1-x-y}\text{Ge}_x\text{C}_y/\text{Si}$  superlattices. Contrast within the  $\text{Si}_{1-x-y}\text{Ge}_x\text{C}_y$  layers and roughening of the interfaces for the case in which Si was grown on  $\text{Si}_{1-x-y}\text{Ge}_x\text{C}_y$  are seen for sample HA96.017, but not for HA97.020.

be quite uniform and the interfaces, abrupt. The interfaces in HA96.017 are sharp only for the case where  $\text{Si}_{1-x-y}\text{Ge}_x\text{C}_y$  was grown on Si. These observations were confirmed by RHEED studies of the growing  $\text{Si}_{1-x-y}\text{Ge}_x\text{C}_y$  layers for which the patterns became spotted. No such spottiness was observed at these compositions for samples grown using the SiC source.

At higher C concentrations, even growth using the SiC source becomes problematic, although the results still represent an improvement over the graphite source. For the case of a 23% Ge, 2.5% C superlattice (composition estimated from analysis of a previous sample), the RHEED pattern at the end of the last period was spotted, indicating a rough surface. There were no peaks observed in HRXRD and so we concluded that the sample must have contained a high density of stacking defects (although the material was basically single crystal). Growth at these compositions using graphite, without the surfactant, had typically resulted in amorphous films.

## B. Surfactant-mediated growth of high-Ge, high-C content superlattices using the SiC source

As we found with the graphite source, growing  $\text{Si}_{1-x-y}\text{Ge}_x\text{C}_y$  at compositions in excess of 20% Ge and 2% C requires the use of a surfactant to stabilize the surface and enhance uniform incorporation of the constituents. For the following, all samples received 1/2 ML Sb predeposit prior to growth of the first  $\text{Si}_{1-x-y}\text{Ge}_x\text{C}_y$  layer. Two series of samples were grown at 500 °C at nominal  $\text{Si}_{1-x-y}\text{Ge}_x\text{C}_y$  deposition rates of 0.1, 0.5, and 1.0 nm/s in order to determine the dependence of growth rate on material quality and substitutional C fraction at higher Ge and C concentrations. Compositions were selected near the condition for perfect lattice match (approximately 9.4:1 Ge:C ratio) and about

which we had previously found stacking fault defects began to appear. These nominal concentrations were 25% Ge/2.5% C for the first series and 25% Ge/2.0% C for the second series.

In the first series (samples not listed in Table I), we found that at a  $\text{Si}_{1-x-y}\text{Ge}_x\text{C}_y$  growth rate of 0.1 nm/s, the RHEED pattern after the last Si layer was spotted, indicating that the layers were single crystal. Further analysis with HRXRD and TEM confirmed that a very high density of stacking defects was present. At 0.5 nm/s, the RHEED pattern disappeared entirely before growth of the superlattice was completed, indicating that the layers were amorphous. An attempt to grow this composition at 1.0 nm/s was deemed unnecessary since increasing the growth rate had been found to produce an amorphous structure.

In the second series, we reduced the C flux slightly and obtained the results shown in Table I for samples HA97.106, .111, and .115. In Fig. 3(a), we show a cross-sectional TEM micrograph from sample HA97.106. HRXRD/RBS analysis determined the Ge and C concentrations in the  $\text{Si}_{1-x-y}\text{Ge}_x\text{C}_y$  layers to be  $30.6 \pm 1.3\%$  and  $2.17 \pm 0.14\%$ , respectively. The uncertainties reflect those associated with the four inputs to the calculation, propagated independently and then summed in quadrature. The analysis also determined the  $\text{Si}_{1-x-y}\text{Ge}_x\text{C}_y$  growth rate to be  $0.090 \pm 0.003$  nm/s. The sample is free of extended defects and inhomogeneities over an interface length scale of approximately 100  $\mu\text{m}$ , resulting in an upper limit on the defect density of  $10^7 \text{ cm}^{-2}$ .<sup>16</sup>

In Fig. 3(b), we show SIMS profiles for Si, Ge, and C as a function of depth into sample HA97.106. As mentioned earlier, HA97.055 was used as a calibration standard for the purpose of converting the raw SIMS data (counts) into concentrations. By averaging the data shown in Fig. 3(b) over the first three superlattice layers, we calculated a value of  $3.42 \pm 1.16$  at. % for the total C concentration. This compares to a value of  $3.62 \pm 1.21$  for HRXRD/CRBS analysis of the sample directly. The percentage of substitutional C was then determined by taking the ratio of the substitutional C concentration (measured by HRXRD/RBS) and the total C concentration (measured by HRXRD/CRBS), yielding  $62 \pm 22\%$ .

## C. Results from substitutional C fraction vs growth rate experiments

Two additional samples were grown in the second series and received approximately the same substitutional C concentration as HA97.106. The growth rate was increased to 0.5 nm/s in sample HA97.111 and finally, to 1.0 nm/s in sample HA97.115. As mentioned previously, TEM micrographs revealed HA97.106 to be free from defects. However, samples .111 and .115 showed signs of a breakdown in epitaxial quality as increasing numbers of stacking faults and threading dislocations were found as the growth rate was increased. HA97.111 and .115 were analyzed for composition, in the same manner as for HA97.106. The results are shown in Table I. In Fig. 4(a), we have plotted the substitutional C fraction as a function of growth rate for samples HA97.055, .106, .111, and .115. The large uncertainties as-

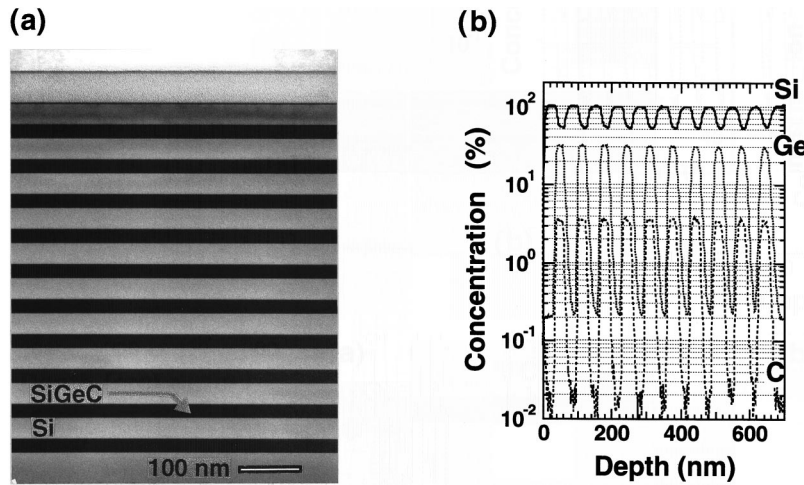


FIG. 3. Cross-sectional TEM micrograph and SIMS profile from sample HA97.106, a 33 nm Si/22 nm  $\text{Si}_{0.672}\text{Ge}_{0.306}\text{C}_{0.022}$  superlattice grown using the graphite source. In (a), a TEM micrograph taken from sample HA97.106 demonstrates that perfect structural quality was obtained at a composition of 31% Ge and 2.2% C using the silicon-carbide source. 1/2 ML Sb was deposited on a Si buffer layer prior to growth of the first  $\text{Si}_{1-x-y}\text{Ge}_x\text{C}_y$  layer. (b) SIMS data showing Si, Ge, and C concentrations vs depth for the sample in (a) are plotted. The data were calibrated using HA97.055 as a standard, characterized for composition by HRXRD/RBS/CRBS.

sociated with the data arise primarily from the difficulty in obtaining an accurate measurement of the total C concentration by CRBS. We found that we could eliminate much of the uncertainty and obtain a relative measure of the substitutional C fraction by plotting the substitutional C concentration divided by the relative count rate for C in the  $\text{Si}_{1-x-y}\text{Ge}_x\text{C}_y$  layers to Si in the Si layers [ $\% C_s / (N_C / N_{\text{Si}})$ ] as measured by SIMS [Fig. 4(b)]. The data show that the substitutional C fraction decreases to a level of approximately 86% of the starting value (from roughly 60% to about 50%) with increasing  $\text{Si}_{1-x-y}\text{Ge}_x\text{C}_y$  growth rate.

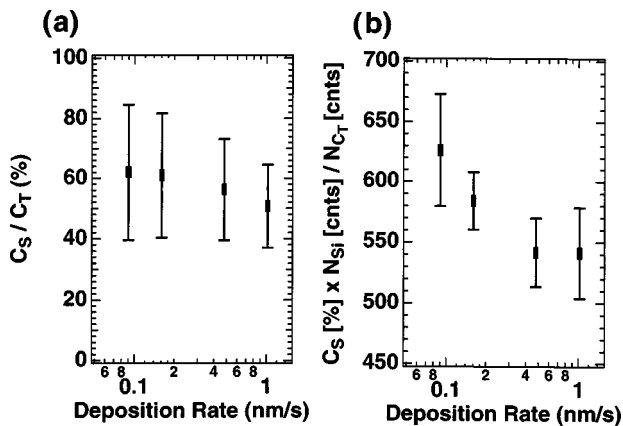


FIG. 4. Plot of substitutional carbon fraction for several samples vs  $\text{Si}_{1-x-y}\text{Ge}_x\text{C}_y$  growth rate. (a) The substitutional C fraction, obtained by dividing the substitutional C concentration (measured by HRXRD/RBS) by the total C concentration (measured by CRBS) is plotted vs  $\text{Si}_{1-x-y}\text{Ge}_x\text{C}_y$  deposition rate for several samples. The error bars on the data arise primarily from uncertainty in the CRBS measurement of the average C concentration. In (b), we obtained a relative measure of the substitutional C fraction using the raw data from SIMS depth profiles performed on the four samples. The data represented are now only proportional to the substitutional C fraction, yet the uncertainty has been reduced to such an extent that a trend toward lower substitutional fractions at higher growth rates can be identified.

#### IV. CONCLUSION

We have studied the growth of  $\text{Si}_{1-x-y}\text{Ge}_x\text{C}_y/\text{Si}$  superlattices by solid-source MBE through the use of a SiC source for C. Sample composition and thickness information obtained by HRXRD, RBS, CRBS, and SIMS were used to develop an understanding of the role of growth rate on crystalline quality and substitutional C fraction, with and without the use of Sb surfactant mediation. At 10% Ge/1% C (substitutional),  $\text{Si}_{1-x-y}\text{Ge}_x\text{C}_y/\text{Si}$  superlattices were found by TEM to grow defect-free, without the need for Sb-surfactant mediation. The constituent Ge and C atoms incorporated in a more uniform manner, as compared with similar samples grown using a graphite source. For Ge and C concentrations approaching 25% Ge and 2.5% C, growth without surfactant mediation resulted in amorphous films. At slightly lower C concentrations, we found that defect-free material could be grown using 1/2 ML predeposit of Sb prior to growth of the superlattices. For Sb-mediated samples, we found that at higher growth rates, crystalline quality became degraded, and the substitutional C fraction decreased slightly. The SIMS data provided a measurement of the relative decrease in substitutional C:  $\sim 86\%$  as much at 1.0 nm/s than at 0.1 nm/s. The absolute substitutional fraction is less accurately known, due to the larger uncertainty associated with the CRBS measurement. We measured a C substitutional fraction of  $62 \pm 22\%$  at 0.09 nm/s using the SiC source.

#### ACKNOWLEDGMENT

Partial support for this work was provided by the Defense Advanced Research Projects Agency (DARPA) monitored

by Lt. Col. Gernot Pomrenke under Contract No. MDA972-95-3-0047.

Presented at the Silicon Heterostructures Conference, Barga, Italy, 15–19 September 1997.

<sup>1</sup>S. Furakawa, H. Etoh, A. Ishizaka, and T. Shimada, U.S. Patent No. 4 885 614 (1989).

<sup>2</sup>R. A. Soref, *J. Appl. Phys.* **70**, 2470 (1991).

<sup>3</sup>B. L. Stein, E. T. Yu, E. T. Croke, A. T. Hunter, T. Laursen, A. E. Bair, J. W. Mayer, and C. C. Ahn, *Appl. Phys. Lett.* **70**, 3413 (1997).

<sup>4</sup>D. L. Harame, J. M. C. Stork, B. S. Meyerson, K. Y.-J. Hsu, J. Cotte, K. A. Jenkins, J. D. Cressler, P. Restle, E. F. Crabbé, S. Subbanna, T. E. Tice, B. W. Scharf, and J. A. Yasaitis, *Tech. Dig. Int. Electron Devices Meet.*, 71 (1993).

<sup>5</sup>E. Kasper, A. Gruhle, and H. Kibbel, *Tech. Dig. Int. Electron Devices Meet.*, 79 (1993).

<sup>6</sup>K. Eberl, S. S. Iyer, S. Zollner, J. C. Tsang, and F. K. LeGoues, *Appl. Phys. Lett.* **60**, 3033 (1992).

<sup>7</sup>K. Eberl, S. S. Iyer, and F. K. LeGoues, *Appl. Phys. Lett.* **64**, 739 (1994).

<sup>8</sup>K. Rim, J. Welser, and J. L. Hoyt, *Tech. Dig. Int. Electron Devices Meet.*, 517 (1995).

<sup>9</sup>K. Ismail, *Tech. Dig. Int. Electron Devices Meet.*, 509 (1995).

<sup>10</sup>E. T. Croke, A. T. Hunter, C. C. Ahn, T. Laursen, D. Chandrasekhar, A. E. Bair, David J. Smith, and J. W. Mayer, *J. Cryst. Growth* **175/176**, 486 (1997).

<sup>11</sup>H. J. Osten, E. Bugiel, and P. Zaumseil, *J. Cryst. Growth* **142**, 322 (1994).

<sup>12</sup>E. T. Croke, A. T. Hunter, P. O. Pettersson, C. C. Ahn, and T. C. McGill, *Thin Solid Films* **294**, 105 (1997).

<sup>13</sup>D. C. Streit and F. G. Allen, *J. Appl. Phys.* **61**, 2894 (1987).

<sup>14</sup>A. R. Verma and P. Krishna, *Polymorphism and Polytypism in Crystals* (Wiley, New York, 1966), p. 99.

<sup>15</sup>J. S. Speriosu and T. Vreeland, *J. Appl. Phys.* **56**, 1591 (1984).

<sup>16</sup>The defect density of  $<1 \times 10^7 \text{ cm}^{-2}$  was calculated based on the assumption that the TEM sample was 100 nm thick and that we had observed defect-free material over approximately 100  $\mu\text{m}$  of interface.